

GRAVITY MODELLING OF SALT DOMES AND PINNACLE REEFS¹

ALEXANDER J.O. JENKINS^{2,3}, DERBEW MESSFIN^{2,4} AND WOOL MOON²

ABSTRACT

Gravity modelling is approached in a slightly different manner in that the density distribution of the body is continuously varying rather than constant. For bodies with cylindrical symmetry, the density contrast function is interpolated by piecewise continuous cubic polynomial basis functions between the data points. The problem is approached, following Parasnis (1961), by first calculating the gravitational attraction of a circular lamina and then integrating this expression over the length of the vertical cylinder. Numerical examples are given for a hypothetical pinnacle reef and salt dome.

INTRODUCTION

Modelling the gravity anomalies due to geologic features has been traditionally achieved by matching these anomalies with the gravitational attractions of simple geometric shapes such as spheres and cylinders. For example, geological features such as salt domes, reefs and igneous plutons have been approximated as cylinders. The gravitational attraction of a cylinder is easily calculated for points on the axis of the cylinder. For points not on that axis, the gravitational attraction is more complicated. This research will follow the general steps devised by Parasnis (1961).

In all previous methods that model the gravitational attraction of cylindrically symmetrical bodies, the density contrast between the host rocks has remained constant. This is rarely the case in geological features, since density is a function of lithology, mineralogy, depth of burial, porosity and other characteristics. This fact produces gravity anomalies that are much different from those due to cylindrical bodies with constant density. Therefore, the provision is made in this paper, following Moon (1981), for density to vary along the radius of a cylindrically symmetrical body. The density function is also allowed to vary along the length of a vertical cylinder. The gravity anomaly due to a cylindrically

symmetrical body with density varying as a function of radius r and depth z is then calculated.

In the following sections, numerical examples for a hypothetical salt dome and pinnacle reef are given. The density contrast in these examples varies with the coordinate variables r and z in a cylindrical coordinate system. The density function is interpolated from data points by using a piecewise continuous cubic polynomial basis function. This makes it possible to calculate the gravitational attraction analytically between the data points and then sum all these results to obtain the total gravitational attraction.

GEOLOGY OF SALT DOMES AND PINNACLE REEFS

In this section, the geology of the two hypothetical examples is discussed. Both these geological features have cylindrical symmetry and the potential to contain oil and gas, so that they have very important implications in hydrocarbon exploration.

SALT DOMES

Salt domes are diapiric structures involving the upward flow of low-density salt. The circular nature of these features is an indication of the fact that salt domes form as a result of upward flow independent of tectonic activity. The flanks of these structures provide excellent trapping mechanisms for oil and gas.

For salt domes to form, thick accumulations of salt must be overlain by sediments of higher density. The exact origin of such a large quantity of salt is not fully understood; however, it is thought that some kind of closed basin of sea water that evaporates is the major mechanism involved. The salt is then buried under unconsolidated Mesozoic and Cenozoic sediments. Nettleton (1934) showed that salt can flow because of the gravitative instability present when salt is overlain by a thick sequence of higher-density sediments. The key here is that salt begins to flow at relatively low temperatures and pressures. Whereas the density of the

¹This material was presented orally by Derbew Messfin and Wool Moon at the annual C.S.E.G. conference (1982) in Calgary, Alberta

²Dept. of Earth Sciences, The University of Manitoba, Winnipeg, Man. R3T 2N2

³Now with Dome Petroleum Ltd., Calgary, Alberta

⁴Now with Geological Survey of Ethiopia, Addis Ababa, Ethiopia

This research is supported by NSERC (Canada) operating grant A-7400 and by University Research Grants (Esso Resources Ltd.).

salt (2.2 g/cm) does not vary with depth, that of the overlying sediments increases because of increasing compaction. This fact causes a positive density contrast at very shallow depths, and an increasingly negative density contrast between the salt and the surrounding sediments as depth increases. Therefore, in modelling the gravitational attraction of a cylindrically symmetrical vertical salt dome, we must use a cylinder whose density is a function of depth rather than one whose density is constant.

The result of the upwelling salt is a structure that truncates beds and also causes a general antiformal trapping mechanism. Since salt is a very tight barrier to hydrocarbon migration, many traps are formed in the bowed-up beds that surround the salt dome. Traps can also be found in the antiformal structure above the dome if impermeable cap rocks with positive density contrasts are present.

PINNACLE REEFS

The other numerical model considered in this study is that of a cylindrically symmetrical pinnacle reef. Reefs of this kind were discovered by Chevron in 1975 as a result of geophysical exploration (specifically, seismic surveys) in the West Pembina area near Edmonton. These "Zeta Lake" reefs are Upper Devonian in age and are composed predominantly of dolomite.

Many wells drilled by Chevron in the West Pembina area have intersected isolated "Zeta Lake" reefs (Chevron, 1979). A type section well has been logged and cored and analysis of these data shows that quartz silt, anhydrite, and clay are all present in minor amounts, with dolomite being the main constituent. Oil has migrated into the porous reef structures and has been trapped by the impermeable sediments overlying the reef. The very fossiliferous dolomite has undergone extreme diagenetic alterations which have determined reservoir characteristics. The main type of porosity is vuggy and the average porosity is 11.5%. Average permeability is 1.5 D. The general shape and dimensions of the reefs are shown in Figure 3a.

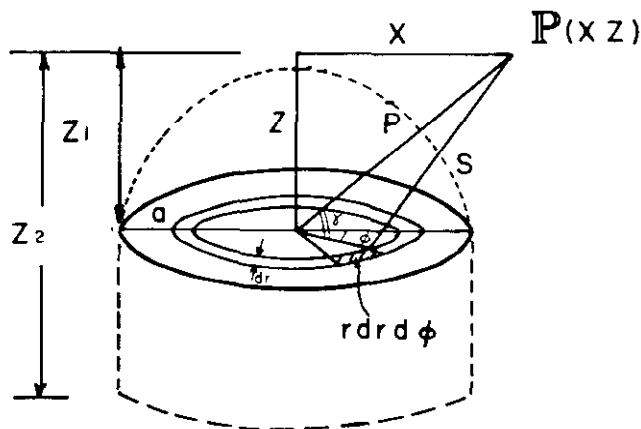


Fig. 1. Cylindrical coordinate system used for calculating the gravitational attraction of a circular lamina and of a right vertical cylinder.

THEORY

To develop the expression for the gravitational attraction of a vertical cylinder whose density is not uniform throughout, we first consider a circular lamina whose surface density varies with its radius *r* (see Fig. 1).

Following Parasnis (1961), the attraction of the element *rdrdφ* is

$$\frac{G\sigma(r)rdrd\phi}{S^2}$$

along the line *S*. The vertical component is

$$\frac{G\sigma(r)rdrd\phi}{S^2} \frac{z}{S}$$

The anomaly due to the entire lamina is

$$\Delta g = \int_0^a \int_0^{2\pi} \frac{Gz\sigma(r)rdrd\phi}{S^3} \tag{1}$$

Also, from the geometry of Figure 1

$$\cos\phi = \frac{x \cos\phi}{p}$$

Note that $s = \sqrt{r^2 - 2rp \cos\phi + p^2}$

$$\text{and } \frac{1}{S^3} = \frac{1}{p^3} \left[\frac{p}{r} P_0'(\cos\phi) + P_1'(\cos\phi) + \frac{r}{p} P_2'(\cos\phi) + \dots \right] \tag{2a}$$

$$\text{or } \frac{1}{S^3} = \frac{1}{r^3} \left[\frac{r}{p} P_0'(\cos\phi) + P_1'(\cos\phi) + \frac{p}{r} P_2'(\cos\phi) + \dots \right] \tag{2b}$$

This is because *S* is the Green's function satisfying the Laplace equation, and hence can be written in terms of the Legendre functions (Morse and Feshbach, 1953, p. 589, 748). *P'_n(cos γ)* are the derivatives of the Legendre polynomials. The integrals from 0 to 2π of the even-order derivatives (*P'₀'*, *P'₂'*, *P'₄'* etc.) are zero since these polynomials contain only odd powers of cos φ. Therefore, the only contributing terms to the integral involve *P'_{2n+1}'(cos γ)*. From the elementary expression for *P_n(cos γ)*

$$P'_{2n+1}(\cos\phi) = \sum_{k=0}^n \frac{(-1)^k 1 \cdot 3 \cdot 5 \dots (4n-2k+1) x^{2n-2k} \cos^{2n-2k} \phi}{2^k k! (2n-2k)!} \tag{3}$$

Since there is a singularity at *S* = 0 (where the material point coincides with the observation point), we must divide the gravitational attraction formulation into two regions: *p* ≥ *a* and *p* ≤ *a*, where *a* is the radius of the circular lamina. For *p* ≥ *a*

$$\Delta g_n = \int_0^a \int_0^{2\pi} \frac{Gz\sigma(r)r}{p^3} (P'_{2n+1}(\cos\phi) \frac{r^{2n}}{p^{2n}}) dr d\phi \tag{4}$$

The general term of gravitational attraction becomes from (3)

$$\Delta g_{nk} = Gz x^{2n-2k} \frac{(-1)^k 1 \cdot 3 \dots (4n-2k+1)}{2^k k! (2n-2k)!} \int_0^a \int_0^{2\pi} \sigma(r) r^{2n+1} \cos^{2n-2k} \phi dr d\phi \tag{5}$$

$$\text{such that } \Delta g = \sum_{n=0}^{\infty} \sum_{k=0}^n \Delta g_{nk} \tag{6}$$

Now for *k* = *n*, the general term only involves *x*⁰. Let Δ*g*₀ denote Δ*g*_{nk}.

$$\begin{aligned} \Delta g_0 &= \frac{Gz}{p^{2n+3}} \sum_{n=0}^{\infty} \frac{(-1)^n 1 \cdot 3 \dots (2n+1)}{2^n n!} \int_0^a \sigma(r) r^{2n+1} dr \int_0^{2\pi} d\phi \\ &= Gz 2\pi \int_0^a \sigma(r) r (r^2 + p^2)^{\frac{n}{2}} dr \end{aligned} \tag{7}$$

Terms with *k* = *n* - 1 involve *x*². Denoting these by Δ*g*₂ and applying the binomial expansion gives

$$\Delta g_2 = \frac{15\pi}{2} Gz x^2 \int_0^a \sigma(r) r^3 (r^2 + p^2)^{\frac{n}{2}} dr \tag{8}$$

Similarly, terms with $k = n - 2$ involve x^4 .

$$\Delta g_n = \frac{2835\pi}{96} G z x^4 \int_0^p \sigma(r) r^5 (r^2 + p^2)^{\frac{11}{2}} dr \quad (9)$$

The integrals in (7), (8), and (9) can be evaluated analytically (Moon, 1981). The other terms in (6) for $k = n - 3, n - 4$, etc. can be obtained similarly.

Consider now the case $p \leq a$, which was not included in the work by Moon (1981). In substituting for $1/S^3$ in (1), there are two distinct cases: $0 \leq r \leq p$ and $p \leq r \leq a$. Therefore the integral in (1) with respect to r becomes

$$\int_0^a = \int_0^p + \int_p^a$$

The first integral on the right hand side is the case we have just evaluated, and equations (7), (8) and (9) can be used to evaluate it. The second integral must be evaluated by substituting (2b) into (1) for $1/S^3$. This gives

$$\Delta g_n = G z \int_p^a \int_0^{2\pi} \sigma(r) P_{2n+1}^1(\cos \gamma) \frac{p^{2n}}{r^{2n+2}} dr d\phi$$

with the general term from (3)

$$\Delta g_{n,k} = G z x^{2n-2k} \frac{p^{2k} (-1)^{2k} 1 \cdot 3 \cdots (4n-2k+1)}{2^k K! (2n-2k)!} \int_p^a \int_0^{2\pi} \frac{\sigma(r) \cos^{2n-2k} \phi}{r^{2n+2}} dr d\phi \quad (10)$$

Proceeding as before

$$\Delta g_0 = 2\pi G z \sum_{n=0}^{\infty} \frac{(-1)^n 1 \cdot 3 \cdots (2n+1)}{2^n n!} \int_p^a \sigma(r) \frac{p^{2n}}{r^{2n+2}} dr \quad (11)$$

$$= 2\pi G z \int_p^a \sigma(r) r (r^2 + p^2)^{\frac{3}{2}} dr$$

$$\Delta g_2 = \frac{15\pi}{2} G z x^2 \int_p^a \sigma(r) r^3 (r^2 + p^2)^{\frac{7}{2}} dr \quad (12)$$

$$\Delta g_4 = \frac{2835\pi}{96} G z x^4 \int_p^a \sigma(r) r^5 (r^2 + p^2)^{\frac{11}{2}} dr \quad (13)$$

The total attraction for $p \leq a$ is the sum of (7), (8) and (9) (with the upper limit of integration being p instead of a with (11), (12) and (13)). Note that the integrands in each case have exactly the same form.

For a cylindrical model we replace $\sigma(r)$ by $\rho(r, z)$ and integrate with respect to z for the length of the cylinder (from z_1 to z_2). The density function $\rho(r, z)$ is a polynomial in r and z . Expressions for Δg_0 , Δg_2 , and Δg_4 become

$$\Delta g_0 = 2\pi G \int_0^a \int_{z_1}^{z_2} \rho(r, z) r (r^2 + p^2)^{\frac{3}{2}} z dz dr \quad (14)$$

$$\Delta g_2 = \frac{15\pi}{2} G x^2 \int_0^a \int_{z_1}^{z_2} \rho(r, z) r^3 (r^2 + p^2)^{\frac{7}{2}} z dz dr \quad (15)$$

$$\Delta g_4 = \frac{2835\pi}{96} G x^4 \int_0^a \int_{z_1}^{z_2} \rho(r, z) r^5 (r^2 + p^2)^{\frac{11}{2}} z dz dr \quad (16)$$

The reason why only Δg_0 , Δg_2 and Δg_4 have been calculated is that numerical testing has shown that the infinite series (6) is a very rapidly converging series.

INTERPOLATION AND NUMERICAL EXAMPLES

ONE-DIMENSIONAL INTERPOLATION

The expressions in equations (7), (8), (9), (11), (12) and (13) all involve the integral of $\sigma(r)$ with respect to r . In practice we do not know the form of $\sigma(r)$ and there-

fore cannot integrate it. However, we can represent $\sigma(r)$ by using continuous basis functions if we have some knowledge of the density at points throughout the circular lamina. Cubic splines will be the type of piecewise continuous basis functions used to interpolate the density function.

Given a set of data points $[r_i, \sigma(r_i)]$, $i = 0, 1, 2, \dots, N$, we can develop cubic polynomials in r in each model interval (r_i, r_{i+1}) . By requiring that these cubics and their first derivatives match at each of the $N - 1$ interior points, we can completely determine each of the cubic splines in each interval (r_i, r_{i+1}) . We need only specify some arbitrary end conditions on the polynomials at r_0 and r_N . The density function is now represented by a cubic polynomial between each data point and the next, and thus can be integrated analytically in all the intervals (r_i, r_{i+1}) . Note that since the cubic splines and their derivatives match at each data point, the density function assumes a very smooth nature. Consequently, the integrals in equations (7), (8), (9), (11), (12) and (13) involve $\sigma(r)$ and a simple function of r , so they can be evaluated analytically for each of the $N - 1$ intervals and summed to obtain the values of Δg_0 , Δg_2 and $\Delta g_4, \dots$

TWO-DIMENSIONAL INTERPOLATION

To evaluate the expressions in equations (14), (15) and (16) we need to integrate the two-dimensional density distribution $\rho(r, z)$. The data required to interpolate this function are a two-dimensional set: $[r_i, z_j, \rho(r_i, z_j)]$, $i = 0, 1, 2, \dots, N, j = 0, 1, 2, \dots, M$. By using the same analysis described above for one-dimensional interpolation, splines can be obtained in the r and z variables. The tensor product of these two multiplied by a characteristic constant for each cell (two-dimensional interval) gives the two-dimensional cubic spline. Therefore, the density function $\rho(r, z)$ becomes a polynomial in r and z in each cell $(r_i, r_{i+1}; z_j, z_{j+1})$. Thus the integrands in (14), (15) and (16) can be evaluated analytically for each cell, and all these results can be summed to obtain the final result for Δg_0 , Δg_2 , etc.

NUMERICAL EXAMPLES

The model used for the salt domes is adapted from Nettleton (1962). His model includes a high-density cap rock such as anhydrite or limestone, which is present above the salt dome and produces a small positive gravity anomaly at the centre of the broad negative anomaly. The gravity anomaly due to a cylindrical salt dome was calculated by using solid angles before the use of computers became prevalent.

A numerical model of the gravitational attraction of a hypothetical cylindrical salt dome is shown in Figure 2a.

The salt dome has a continuously varying density distribution $\rho(r, z)$ which was interpolated by cubic

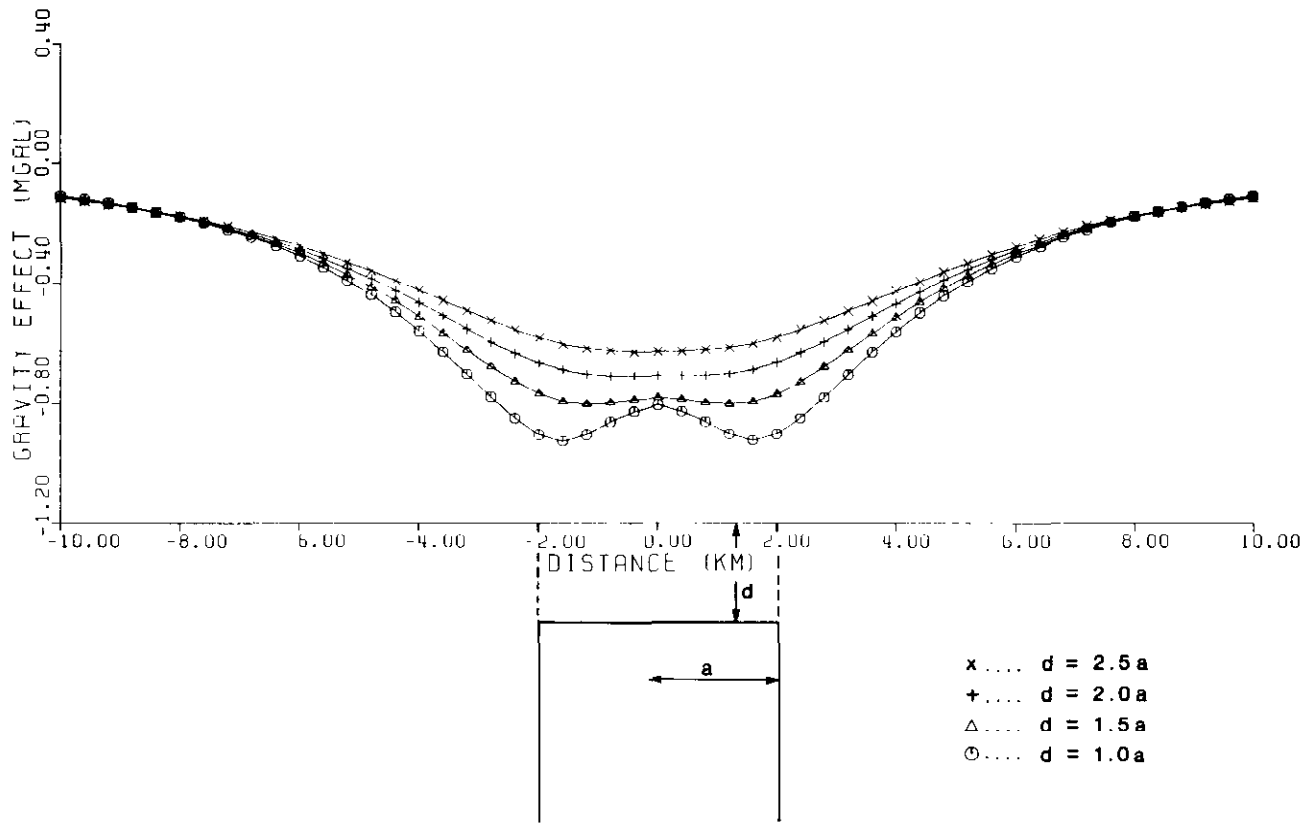


Fig. 2a. Gravity anomaly due to a cylindrically symmetrical hypothetical salt dome in various geometries.

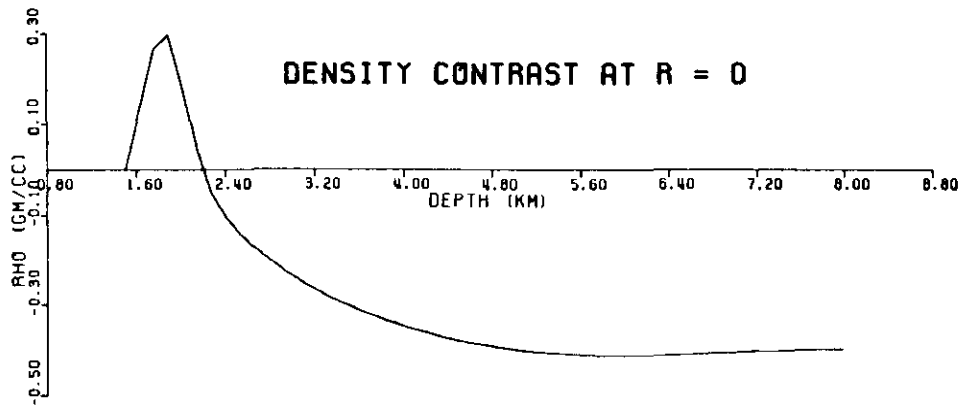
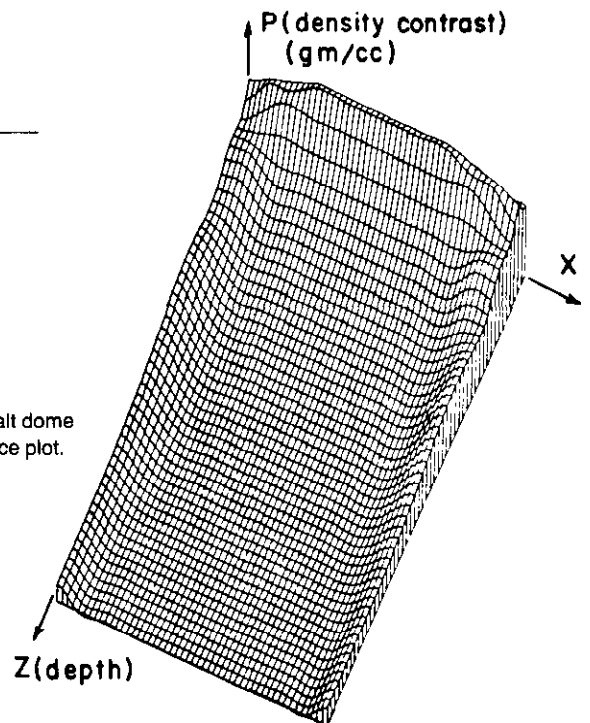


Fig. 2b. Density contrast profile as a function of depth.

Fig. 2c. General shape of salt dome and its density contrast surface plot.



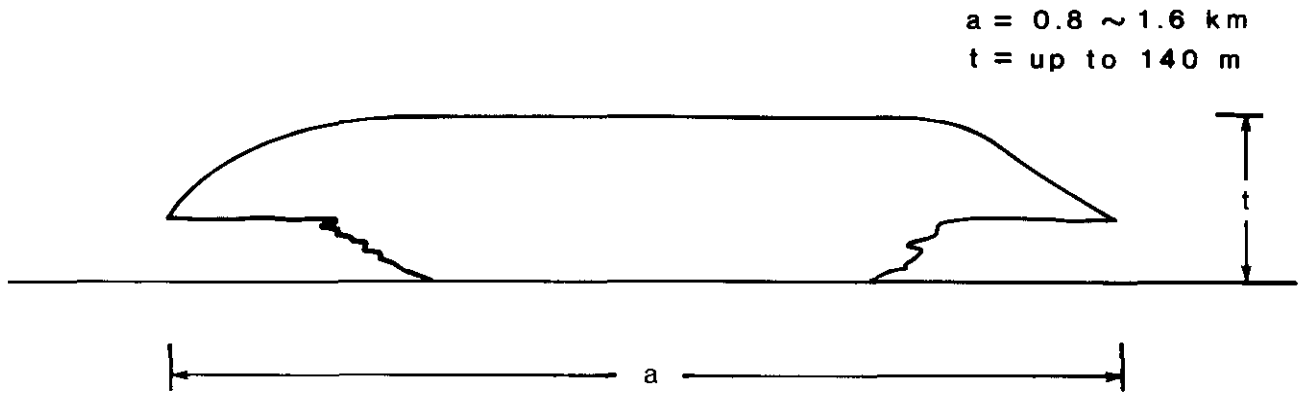


Fig. 3a. Diagrammatic section of a Zeta Lake pinnacle reef.

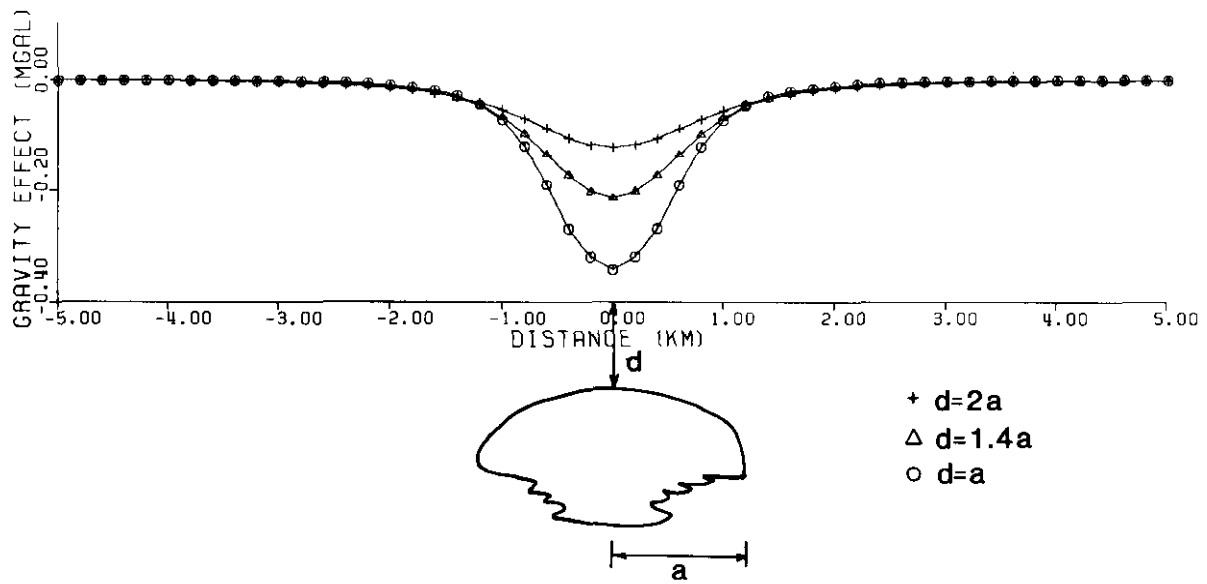


Fig. 3b. Gravity anomalies produced by cylindrically symmetrical hypothetical pinnacle reef in various geometries.

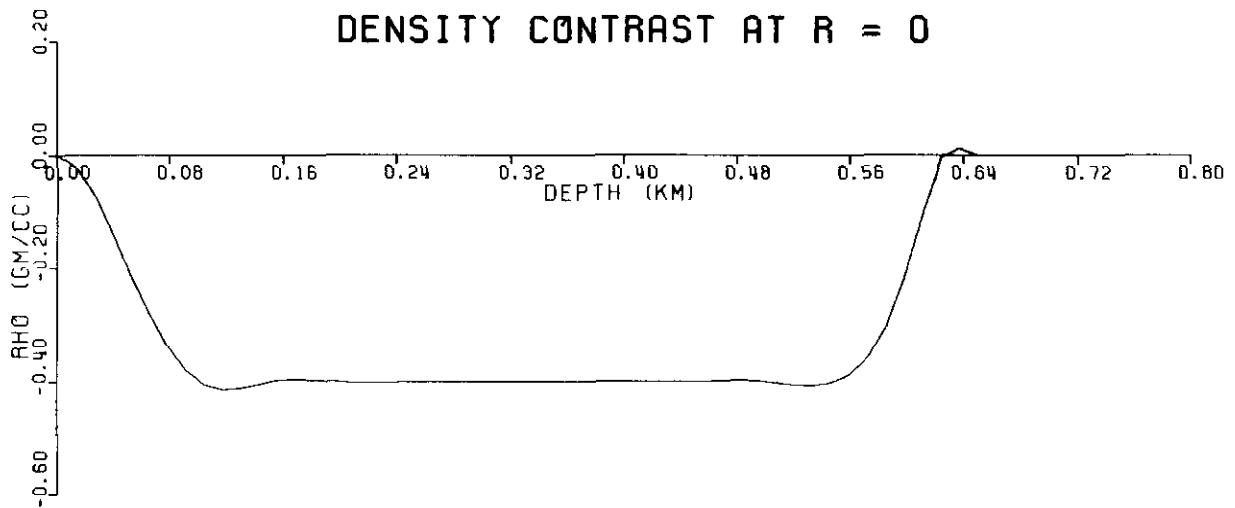


Fig. 3c. Density contrast profile as a function of depth.

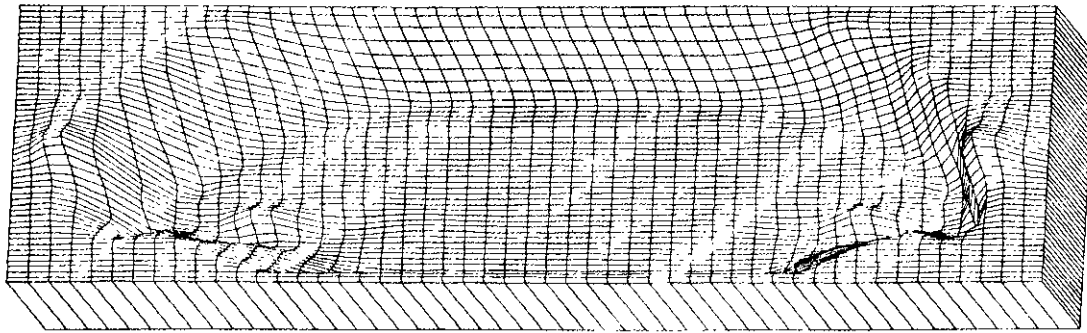


Fig. 3d. General shape of hypothetical pinnacle reef and its density contrast surface plot.

spline functions described earlier. The spline interpolates between the data points $[(r_i, z_j, \rho(r_i, z_j))]$, $i = 0, 1, \dots, N, j = 0, 1, 2, \dots, M$. In practice, the data needed to interpolate the density function can be obtained from well data. Equations (14), (15) and (16) were used to calculate the gravity anomaly.

Figure 2(b) shows the density contrast profile at the centre of the salt dome ($r = 0$) as a function of depth. Figure 2(c) shows the density contrast surface plot of the salt dome.

Figures 3(b)-3(d) show the gravity anomaly of a hypothetical cylindrically symmetrical pinnacle reef, its density contrast profile and its density contrast surface plot. Once again cubic splines were used to interpolate $\rho(r, z)$.

CONCLUSION

The numerical models shown in Figures 2 and 3 demonstrate that it is possible to calculate the gravitational attraction of cylindrically symmetrical objects with continuously varying density functions. We could also have interpolated the density function with a piecewise continuous basis function to accommodate any jump discontinuities in the density distribution. Cubic polynomials were used in this study to interpolate the density functions of these models; however, one can also use other types of piecewise continuous basis functions. One possible practical application of this method could

be in the exploration for structures that contain hydrocarbons, such as salt domes and reefs.

REFERENCES

- Exploration staff, Chevron Standard Limited, 1979, The geology, geophysics and significance of the Nisku reef discoveries, West Pembina area, Alberta, Canada: Bulletin of Canadian Petroleum Geology, v. 27, p. 326-359.
- Gerald, Curtis F. 1980, Applied Numerical Analysis. Don Mills, Ontario: Addison-Wesley Publishing Company.
- Hunt, John M. 1979, Petroleum Geochemistry and Geology. San Francisco: W.H. Freeman.
- Moon, Wooil 1981, A new method of computing geopotential fields: Geophys. J.R. astron. Soc., v. 67.
- Morse, P.M. and Feshbach, H. 1953, Methods of Theoretical Physics. New York: McGraw-Hill Book Company.
- Nettleton, L.L. 1934, Fluid mechanics of salt domes: Am. Assoc. Petroleum Geologists Bull., v. 18, p. 1175-1204.
- _____. 1962, Gravity and magnetics for geologists and seismologists. Am. Assoc. Petroleum Geologists Bull., v. 41, p. 1815-1838.
- Parasnis, D.S. 1961, Exact expression for the gravitational attraction of a circular lamina at all points of space and of a right vertical cylinder at points external to it: Geophys. Prosp., v. 9, p. 382-398.
- Schultz, Martin H. 1973, Spline Analysis. Englewood Cliffs, N.J.: Prentice-Hall, Inc.
- Spencer, Edgar W. 1977, Introduction to the Structure of the Earth. New York: McGraw-Hill Book Company.
- Stacy, Frank D. 1977, Physics of the Earth. New York: John Wiley and Sons.
- Telford, W.M. *et al.* 1976, Applied Geophysics. Cambridge: Cambridge University Press.